

Personalization of Cardiac Electrophysiology Model using the Unscented Kalman Filtering

Hugo Talbot, Stephane Cotin, Reza Razavi, Christopher Rinaldi, Hervé
Delingette

► **To cite this version:**

Hugo Talbot, Stephane Cotin, Reza Razavi, Christopher Rinaldi, Hervé Delingette. Personalization of Cardiac Electrophysiology Model using the Unscented Kalman Filtering. Computer Assisted Radiology and Surgery (CARS 2015), Jun 2015, Barcelona, Spain. hal-01195719

HAL Id: hal-01195719

<https://hal.inria.fr/hal-01195719>

Submitted on 10 Nov 2015

HAL is a multi-disciplinary open access archive for the deposit and dissemination of scientific research documents, whether they are published or not. The documents may come from teaching and research institutions in France or abroad, or from public or private research centers.

L'archive ouverte pluridisciplinaire **HAL**, est destinée au dépôt et à la diffusion de documents scientifiques de niveau recherche, publiés ou non, émanant des établissements d'enseignement et de recherche français ou étrangers, des laboratoires publics ou privés.

Personalization of Cardiac Electrophysiology Model using the Unscented Kalman Filtering

Hugo Talbot^{1,2}, Stephane Cotin¹, Reza Razavi³, Christopher Rinaldi⁴, Herv Delingette²

¹ INRIA Lille North Europe, France

² INRIA Sophia Antipolis, France

³ Department of Cardiovascular Imaging, King's College, London, United Kingdom

⁴ Department of Cardiology, Guy's and St. Thomas' NHS, London, United Kingdom

Abstract. Cardiac electrophysiology mapping techniques now allow to record denser intra-operative electrograms (ECG). The patient-specific information extracted from these clinical recordings is extremely valuable. A growing field of research focuses on the personalization of electrophysiology models using this patient-specific information. The modeling *in silico* of a patient electrophysiology is needed to better understand the mechanism of cardiac arrhythmia. In the scope of ischemic cardiomyopathy, the predictive power of patient-specific simulations may also provide a substantial guidance in defining the optimal location of the implantable defibrillator, since all possible configurations could be tested *in silico*. This article describes an innovative personalization approach based on an unscented Kalman filter. Following an iterative process, the apparent conductivity is efficiently estimated in specific regions. A sensitivity analysis is performed to assess the filter parameters. With three patient cases, we finally demonstrate the accuracy and efficiency of our algorithm.

Among all cardiovascular diseases, cardiac arrhythmia and heart failure are life-threatening pathologies. Ischemic cardiomyopathy is one of the cause of heart failure: the narrowing or occlusion of a coronary artery causes a myocardial hypoxia, which compromises the heart's ability to efficiently pump blood. Depending on their ventricular function, patients with ischemic cardiomyopathy may benefit from an implantable cardiac defibrillator (ICD) for primary prevention. According to the NICE guidelines [1], an electrophysiology study must be conducted in order to determine if an ICD implant would be tolerated. In this scope, patient-specific simulations may help cardiologists to better interpret the arrhythmic complex. More challenging, these predictive computations could even assist the surgeon in the placement of the ICD leads.

Personalizing a mathematical model consists in estimating the model parameters that best fit experimental or clinical electrophysiology data. If the choice of the algorithm directly impacts the personalization, the choice of the electrophysiology model may also strongly affect the efficiency and the accuracy of the personalization outcome. Mathematical models simulating the cardiac electrophysiology can be sorted into three different classes: (i) biophysical models [2],

which are complex models, involving many parameters and simulating the electrophysiology at the cellular scale; (ii) phenomenological models [3,4], which are simplified models derived from the biophysical models, involving less parameters and capturing the electrophysiology at the organ scale; (iii) Eikonal models [5], which correspond to static non-linear partial differential equations of the depolarization time derived from the previous models. The complex biophysical models imply high computational cost and a lack of observability of the parameters. Modeling the propagation of the action potential without modeling the action potential itself, the Eikonal formulation appears to be unsuitable for arrhythmia prediction due to the complexity of both the refractoriness and the curvature of the wavefront. With an intermediate complexity and a relative computational efficiency, phenomenological models turn out to be an interesting compromise.

Personalization of electrophysiology models assume to fit patient data, such as ECG or electrophysiology mapping. Patient-specific features, such as depolarization times, repolarization times, conduction velocity (CV), action potential duration (APD) and their restitution, must be extracted from this electrophysiology mapping to be used in the personalization process. In this work, our contribution in patient-specific modeling exclusively focuses on the estimation of the apparent conductivity of the ventricles, i.e. the presented model personalization does not cover the estimation of restitution parameters.

The estimation of the cardiac tissue conductivity is crucial for the detection of conduction pathologies. Previous works tackle this optimization problem using various methods. Zettinig et al. [6] propose a calibration of a Mitchell Schaeffer model. The authors first need to couple the 12-lead ECG with the myocardial electrophysiology model, which is implemented using a Lattice-Boltzmann approach. Then, a multivariate polynomial regression estimates the model parameters in the right and left ventricles. Interesting results are shown with a prediction error less than 5 ms for QRS duration, yet the use of thoracic ECG compromises the modeling of local or complex electrophysiology patterns.

In [7], Liu et al. propose a modified formulation of the Nelder-Mead algorithm coupled with a particle swarm optimization. Data acquired on isolated Guinea pig ventricular myocytes are used to assess the algorithm. This work aims at estimating parameters of the Bueno-Orovio phenomenological model, but it provides only few interpretable results. Two studies [8,9] introduce the Powell's method as personalization tool for electrophysiology models. Both rely on an Eikonal model and present an estimation of regional apparent conductivities using non-contact electrophysiological data. Despite the coarseness of the mesh (256 nodes) and the relatively large root mean square error (27 ms), Chinchapatnam et al. [8] present a proof of concept able to simulate a left bundle branch block and the electrical wave propagation for different pacing modes. In 2011, Relan et al. [9] integrate the personalization of the restitution properties: the Eikonal model is used to estimate the conductivity parameters and a Mitchell Schaeffer model is added to capture the restitution properties. Despite the good prediction of the induction of ventricular tachycardia (mean absolute error on depolarization times is about 7.1 ms using the Eikonal model and 18.5 ms using

the Mitchell Schaeffer model), this two-step process does not guarantee to capture the myocardial activity. Estimation of the apparent conductivity requires about 30 to 40 minutes. In [10], Relan et al. concentrate on the personalization of the Mitchell Schaeffer model using optical and MRI data from *ex vivo* porcine heart. In the latest version of this work, the mean absolute error regarding the depolarization time is 8.7 ms and the entire computation requires about 12 hours.

Based on the Eikonal equation solved using the fast marching method, Camara et al. [11] develop a stochastic approach using the genetic algorithm to personalize the fast conduction Purkinje system. The authors thus estimate a regional distribution of Purkinje end-terminals. No computation time is mentioned but Camara et al. reached a mean error of about 17 ms regarding the endocardial activation time. A probabilistic approach of the model personalization using Bayesian inference is preferred in [12]. With a spectral representation based on polynomial chaos expansions, the resulting personalization runs within 5 hours, the root mean square error on endocardial depolarization times is about 15.3 ms and error on epicardial depolarization times amounts to 32.2 ms.

In this paper, we present an efficient method for personalizing the conductivity of the MS model based on dense intra-cardiac recordings. Based on an unscented Kalman filter (UKF), our approach takes into account uncertainties regarding the initial parameters and the clinical data. Applied on the patient data, the method provides accurate results compatible with clinical times.

1 Materials & Methods

1.1 Data Acquisition

In this work, we consider three patients suffering from ischemic cardiomyopathy. All patients underwent an electrophysiology study to determine the effectiveness of an ICD implant. These patient data from Kings College London were made available for research work in the scope of the european project euHeart. This section details how the patient data were acquired and then processed in order to make the model personalization possible.

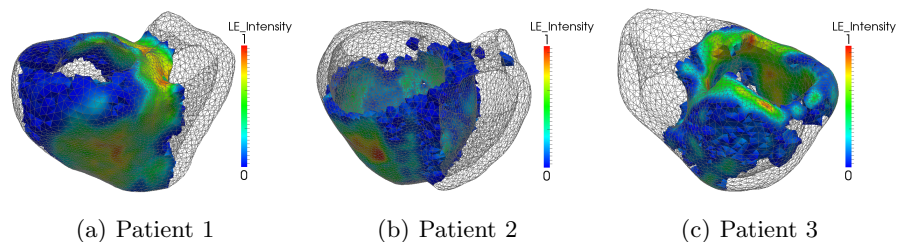


Fig. 1. Unitary intensity of the late enhancement imaging (Gadolinium), characterizing the scars and grey zones, within the generated meshes

Image Processing Two different acquisitions were conducted, both using a Philips Achieva 1.5T. First, the whole cardiac anatomy needs to be reconstructed. To obtain high resolution images, balanced SSFP free-breathing scans were performed for each of the three patients. The isotropic resolution was 1.8 mm^3 and a respiratory motion correction was used for the purpose of segmentation. Second, as all patients present an ischemic cardiomyopathy, a high resolution imaging of the scars is compulsory. The localization of the scars and grey zones (border areas around scars) are key in the arrhythmic mechanism. The grey zones consist in damaged and healthy tissues which make these areas high potential arrhythmogenic substrates. To acquire scars, a gadolinium contrast agent was injected (Gadobutrol 0.2 mmol/kg) and sequences were recorded 20 minutes post intravenous injection with a voxel size $1.3 \times 1.3 \times 2.6 \text{ mm}^3$.

The 3D balanced SSFP images are processed in the open source framework GIMIAS¹ to recover the four chambers of the heart by assigning individual linear transformations to the heart chambers and to the great vessels. The signal intensities included in the late Gadolinium enhancement images allow us to threshold the scars and the grey zone, as shown in Fig. 1.

Mesh Generation To be incorporated in our electrophysiology simulation, all patient hearts must be meshed. We use the open source library CGAL², which allows to mesh labeled masks with heterogeneous element sizes, as illustrated

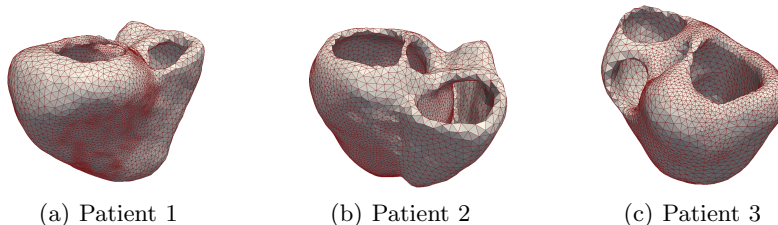


Fig. 2. Adaptive meshes with local refinements in the scar border zones obtained from patient data (SSFP and LGE imaging)

Table 1: Structural information of the heterogeneous patient-specific meshes computed using CGAL

	Patient 1	Patient 2	Patient 3
Number of elements	65,198	67,415	61,557
Number of nodes	14,102	14,914	12,162
Smallest edge size (mm)	0.54	1.45	0.48
Largest edge size (mm)	7.00	8.21	9.60

¹GIMIAS is an open source framework providing image visualization, manipulation, and annotation. For more information: www.gimias.net

²CGAL is an open source software library that provides algorithms in computational geometry. For more information: www.cgal.org

in Fig. 2. Scar information is labeled in the whole heart image provided by the balanced SSFP, so that we obtain adaptive meshes with refinements in the arrhythmogenic grey zones. Table 1 details the structural information of all three meshes.

Electrophysiology Mapping Dense intra-cardiac data were recorded during a non-contact electro-anatomic mapping using a multi-electrode steerable catheter (EnSite Velocity System, St Jude Medical, MN, USA). To reach the LV, the cardiologist must lead the catheter from the femoral artery to the heart via the aorta. Once inside the targeted cardiac chamber, the reconstruction of endocardial electrical potentials can start using the Ensite system. All three patients underwent a ventricular tachycardia (VT) stimulation procedure following the Wellens protocol [13] in order to determine if an ICD should be implanted.

The electrophysiology catheter tracked in the operating room measured unipolar electrograms. The signals were filtered and then exported using the Ensite Velocity System recorder. An offline signal processing was performed to detect the depolarization times from the QRS window and the repolarization times from the ST window. Depolarization times are the intra-operative information used to personalize the model conductivity. Finally, the activation resulting from the stimulation at different pacing frequencies (400, 500 and 600 ms) allows us to establish the relationship between the DI of one cycle and the APD of the following cycle. The non-linear equation representing the restitution curves will be later estimated based on these relationships.

1.2 Personalization based on Data Assimilation

Electrophysiology Model As introduced previously, there exists several models to describe the ventricular action potential. However, biophysical models are complex model involving many parameters and imply an important computational cost. Eikonal models are efficient algorithms but have difficulty to simulate complex electrophysiology phenomena with non-physiological parameters. We therefore choose to rely on a phenomenological model: the Mitchell Schaeffer (MS) model [4]. This model only involves six parameters that can be physiologically identified and even captures the restitution properties of action potential duration.

The MS model, derived from the Fenton Karma model [3], has two variables: u the transmembrane potential and z a secondary variable controlling the repolarization phase. The temporal evolution of these two variables is governed by the following equations:

$$\begin{cases} \partial_t u = \operatorname{div}(D\nabla u) + \frac{zu^2(1-u)}{\tau_{in}} - \frac{u}{\tau_{out}} + J_{stim}(t) \\ \partial_t z = \begin{cases} \frac{(1-z)}{\tau_{open}} & \text{if } u < u_{gate} \\ \frac{-z}{\tau_{close}} & \text{if } u > u_{gate} \end{cases} \end{cases} \quad (1)$$

The diffusion term is defined by an 3x3 anisotropic diffusion tensor $D = d \cdot \text{diag}(1, r, r)$ where d defines the tissue electrical conductivity and r is the transverse anisotropy ratio. The parameters τ_{in} and τ_{out} define the repolarization phase whereas the constants τ_{open} and τ_{close} manage the gate opening or closing depending on the change-over voltage u_{gate} . The contribution of this work resides in the estimation of the patient-specific tissue conductivity d based on the intra-operative map of depolarization times. In this paper, a GPU implementation based on [14] is chosen in order to significantly decrease the computation time.

Choice of the Optimization Method Simulation can provide virtual training for the RF ablation procedure but it also appears to be a promising tool to help cardiologists find the optimal ICD location. In this context, the proposed personalization process must be fast, accurate to reproduce patient’s arrhythmia and must involve as few pre-processing as possible.

Since the depolarization waves can not be assumed as planar, no analytical expression can be established between the depolarization times and the conductivity. As a consequence, algorithms depending on the analytical gradient would not suit our optimization problem. To match the electrophysiology model with the clinical data, samples simulating the depolarization times given a set of conductivities must be computed. Due to the important number of required samples, stochastic approach may result in a time-consuming optimization. All other optimization methods could be chosen in our scope.

In this work, we propose to reformulate the cardiac electrophysiology into a recursive Bayesian representation using a Kalman filter. Characterized by a strongly non-linear activity, the transmembrane potential could not be accurately approximated by the original Kalman or the extended Kalman filter. We choose to rely on the UKF developed by Julier et al. [15], which has many interesting properties. Not only does the UKF handle function non-linearities, but it also presents a low complexity while taking into account model and data uncertainties.

Region Definition The estimation of patient-specific model parameters at each node of the cardiac mesh would imply a huge computational cost. To decrease the number of variables while preserving a spatial accuracy, we estimate the model parameters in regions.

In their latest work [10], Relan et al. base their personalization process on the cardiac zones defined by the American Heart Association. These 17 regions have no physiological meaning regarding the conductivity, and may therefore not be optimal for our problem. Chinchapatnam et al. [8] also personalize regional conductivity using a multi-level decomposition. In this work, we propose to determine the conductivity d of the MS model in regions which are based on the CV, i.e. the velocity of the depolarization wave. Even if no relationship exists between d and CV, creating meaningful regions using CV would speed up the optimization while preserving accuracy.

CV can be extracted by computing the gradient of the clinical depolarization times:

$$CV = \frac{\partial x}{\partial t_{depo}} = (\nabla t_{depo})^{-1} \quad (2)$$

However, the CV information is only available on the endocardium. To define volumetric regions, we extrapolate the CV information through the cardiac wall, by numerically diffusing the CV field through the myocardium. The regions are then computed from the logarithm of CV using an arithmetic progression, i.e. a regular subdivision regarding $\log(CV)$. A logarithmic representation allows to better pack the CV values. Let m be the minimum value of our $\log(CV)$ distribution and M its maximum value. The i^{th} zone corresponds to:

$$m + (i - 1) \cdot \left(\frac{M - m}{N} \right) < \log(CV)_i < m + i \cdot \left(\frac{M - m}{N} \right) \quad (3)$$

where $i \in [1, N]$ and N is the number of regions. In this study, we consider a clustering based on CV involving: four zones and eight zones. Using different numbers of zones enables to analyze their influence on the personalization. The Fig. 3(d) to 3(f) illustrate the four zones generated for each patient case.

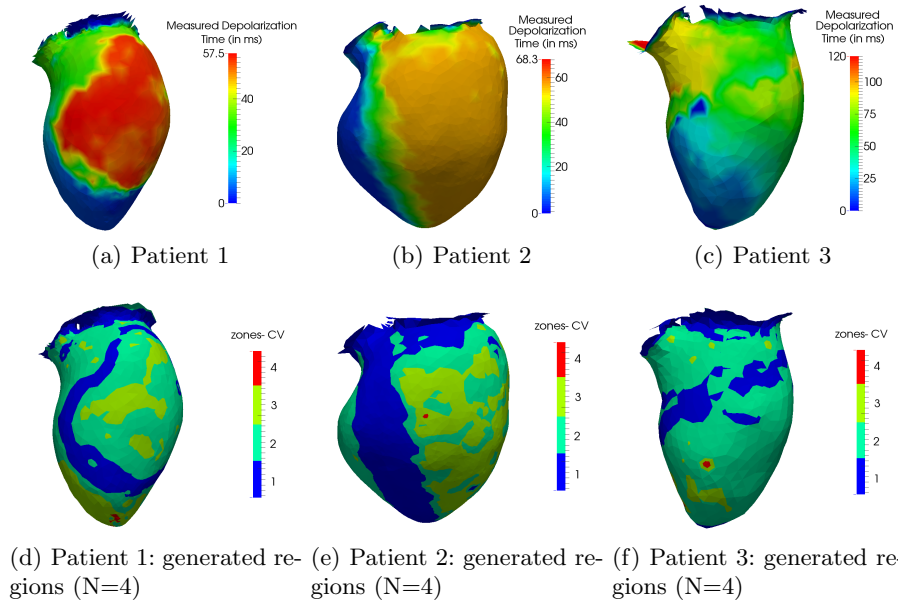


Fig. 3. (a-c) Depolarization times mapped on the patients' endocardium computed from electrophysiology mapping; (d-f) Four regions clustered from the CV information

Restitution Electrophysiological restitution defines the property of cardiac tissue to adapt its electrophysiology depending on the heart rate. The spatial heterogeneity of the restitution properties (especially APD restitution) has a crucial role in arrhythmogenesis. In order to faithfully model the patient’s arrhythmia, the restitution parameters need to be estimated. To do so, we apply the optimization method detailed in [9]. Only APD restitution is computed, i.e. both τ_{open} and τ_{close} are first adjusted on the endocardium to fit the measurements at different pacing frequencies. The ratio $h_{min} = 4(\tau_{in}/\tau_{out})$ is kept to the literature value $h_{min} = 0.2$. The τ_{open} and τ_{close} values are finally diffused in order to obtain smooth restitution parameters within the myocardium.

UKF-Based Personalization

Original UKF The UKF [15] belongs to the sequential data assimilation methods and estimates state variables X of a dynamic system through statistical analysis, each time a new measurement is available. Usually, the state variables depict the position of a system, but it can in fact include model parameters, such as electrical conductivities. The measurements of the observed system Z must be available and are described through the observation operator, noted H , so that: $Z = H(X)$. In the UKF, the estimation \hat{X} of the state variables requires two steps at each measurement time n :

- **Prediction:** it first computes regression points (called sigma-points) corresponding to the minimal set of sample points around the mean. The i^{th} sigma-point is:

$$\hat{X}_n^{(i)+} = \hat{X}_n^+ + \sqrt{P_n^+} I^{(i)} \quad (4)$$

Different types of sigma-points can be created depending on the interpolation rule I chosen. In this work, simplex, canonical and star sigma-points are considered. Each sigma-point is then propagated through the dynamic operator A . The mean \hat{X}_{n+1}^- and *a priori* state covariance P_{n+1}^- of the transformed state can be computed.

$$\begin{cases} \hat{X}_{n+1}^- = E(A_{n+1|n}(\hat{X}_n^+)) \\ P_{n+1}^- = \text{cov}(A_{n+1|n}(\hat{X}_n^+)) \end{cases} \quad (5)$$

- **Correction:** The state vector and its covariance are first updated using the new sigma-points. The corresponding observations \hat{Z}_{n+1} are propagated by the non-linear observation operator H using the noise covariance W_{n+1} . The state correction relies on an innovation term (comparing the measurements Z_{n+1} with the estimated observations \hat{Z}_{n+1}) and on the Kalman gain, noted K . Finally, the *a posteriori* estimate covariance P_{n+1}^+ is updated for the next iteration.

$$\begin{cases} \hat{X}_{n+1}^{(i)-} = \hat{X}_{n+1}^- + \sqrt{P_{n+1}^-} I^{(i)} \\ Z_{n+1}^{(i)} = H_{n+1}(\hat{X}_{n+1}^{(i)-}) \\ P^{XZ} = \text{cov}(\hat{X}_{n+1}^-, \hat{Z}_{n+1}) \\ P^Z = \text{cov}(\hat{Z}_{n+1}, \hat{Z}_{n+1}) + W_{n+1} \\ K_{n+1} = P^{XZ}(P^Z)^{-1} \end{cases} \quad (6)$$

$$\begin{cases} \hat{X}_{n+1}^+ = \hat{X}_n^- + K_{n+1}(Z_{n+1} - E(\hat{Z}_{n+1})) \\ P_{n+1}^+ = P_{n+1}^- - P^{XZ}(P^Z)^{-1}(P^{XZ})^T \end{cases} \quad (7)$$

Modified UKF We present here a modified version of the UKF based on the Verdandi library ⁴. For each patient, the challenge consists in efficiently estimating regional conductivities, so that our simulation fits the depolarization time map recorded intra-operatively. In our application, the state \hat{X} includes the absolute value of the regional conductivities $|d_R|$. Since clinical recordings only provide one set of depolarization times per patient, our modified UKF does not include a dynamic operator A and the prediction steps is simplified as:

$$\begin{cases} \hat{X}_{n+1}^- = E(\hat{X}_n^+) \\ P_{n+1}^- = \text{cov}(\hat{X}_n^+) \end{cases} \quad (8)$$

From a given updated transformed state \hat{X}_{n+1}^- (set of regional conductivities), the simulation computes one cardiac cycle until the whole ventricular myocardium is depolarized. This simulation process corresponds to the non-linear observation model H and returns simulated depolarization times, i.e. the estimated observation vector \hat{Z}_{n+1} . By recursively applying a UKF step on the same measurements, we iteratively optimize the regional conductivities using the intrinsic statistical knowledge of the Kalman gain.

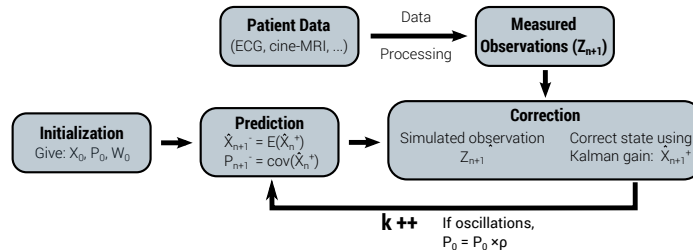


Fig. 4. Structure of our modified UKF applied to our patient data in order to personalize regional conductivities

⁴Verdandi is a generic C++ library developed at INRIA for data assimilation. For more information: verdandi.sourceforge.net

If both confidences in the state and in the observations remain constant over the iterations, the iterative application of our UKF would generate oscillations due to an over-confidence in our measurements. The error variance regarding the state is progressively decreased to increase the confidence in \hat{X} over the iterations. As soon as an oscillation effect is detected, a factor ρ is used to damp the *a priori* state covariance P_0 . Finally, the optimization process ends using either a maximum number of iterations or a tolerance criterion regarding the convergence of \hat{X} . The structure of the entire iterative algorithm is shown in Fig. 4.

Default Numerical Settings Kalman filters are known to be very sensitive to the filter parameters. Moreover, all UKF parameters are cross-related, which makes the calibration delicate. A set of default parameters is defined to analyse the sensitivity of each parameter. For the state, the initial regional conductivity is defined as $X_0 = 5 \cdot 10^{-3} \text{ m}^2/\text{s}$, which over-estimates the CV. By choosing a time step $dt = 10^{-5} \text{ s}$ suitable for this fast depolarization, we make sure that the simulation will remain stable in the remaining iterations. The confidence in the input state is characterized by the *a priori* state covariance $P_0 = 0.2 \text{ m}^4/\text{s}^2$. The noise covariance associated with the recorded depolarization times amounts to $W_0 = 10^{-5} \text{ s}^2$. The damping factor ρ used for a better convergence equals 0.25. The optimization process is controlled by a maximum number of iterations (20 iterations) and a convergence criterion of $\Delta X = |X_{n+1} - X_n| < 10^{-5} \text{ m}^2/\text{s}$. As soon as one of both conditions is reached, the algorithm ends.

2 Results

2.1 Sensitivity Analysis

In this section, the optimization process described previously is applied on the three clinical datasets. A sensitivity analysis is conducted to assess the set of UKF parameters that would suits any patient data. The influence of the initial state, the initial covariances, the sigma-points distribution and the number of regions is studied. Results are evaluated regarding: the error on depolarization times compared to the maximum depolarization time (MDT), the computation time, and the breaking condition: either the number of iterations exceeds 20 ("Iter") or the convergence tolerance is reached ("Tol").

Input state Due to the high sensitivity of the Kalman filters, the influence of the UKF parameters is assessed, starting with the initial state X_0 . Here, the sensitivity analysis is conducted using the patient 1 dataset, using the default numerical settings and four CV-based regions. Three different initial conductivity values are tested and reported in Table 2. The first configuration defines a low conductivity $X_0 = 0.2 \cdot 10^{-3} \text{ m}^2/\text{s}$ in the four regions. The second (*default*) computation uses a high conductivity $X_0 = 5 \cdot 10^{-3} \text{ m}^2/\text{s}$ in the four regions. The third initial state takes advantage of the *a priori* knowledge on the CV-based regions. Since the regions are clustered depending on the local CV, a low

Table 2: Influence of the input state x_0 , including the initial regional conductivities in $10^{-3} \text{ m}^2/\text{s}$ (only on patient 1)

Initial state vector X_0 (m^2/s)	$X_0 = \{0.2, 0.2, 0.2, 0.2\}$	$X_0 = \{5, 5, 5, 5\}$ <i>default</i>	$X_0 = \{2, 4, 6, 8\}$
Mean error (ms)	10.3	9.99	9.99
Max error (ms)	49.7	50.8	49.2
Computation time (min)	28.4	20.5	16.9
Breaking condition	Tol (in 15 iter.)	Tol (in 17 iter.)	Tol (in 13 iter.)

conductivity is associated to the low-CV zone, respectively a high conductivity is set for the high-CV zone. The third state equals $X_0 = \{2, 4, 6, 8\} \cdot 10^{-3} \text{ m}^2/\text{s}$.

Compared to the *default* configuration, using a lower initial conductivity ($X_0 = 0.2 \cdot 10^{-3} \text{ m}^2/\text{s}$) means slower depolarization waves and therefore implies longer computation time per iteration. It also appears that defining an initial state, of which conductivities are related on the measured CV, allows faster convergence rate. The third configuration only requires 16.9 minutes of computation while preserving the estimation accuracy.

Table 3: Influence of the *a priori* state covariance P_0 and the noise covariance W_0 associated with the measurements, starting with $X_0 = \{5, 5, 5, 5\} \cdot 10^{-3} \text{ m}^2/\text{s}$ (only on patient 1)

A priori state covariance P_0 (m^4/s^2)	$P_0 = 0.05$	$P_0 = 0.2$ <i>default</i>	$P_0 = 0.5$
Mean error (ms)	10.9	9.99	9.96
Max error (ms)	50.1	50.8	50.8
Computation Time (min)	18.6	20.5	17.7
Breaking condition	Iter	Tol (in 17 iter.)	Tol (in 15 iter.)
Noise covariance W_0 (s^2)	$W_0 = 10^{-4}$	$W_0 = 10^{-5}$ <i>default</i>	$W_0 = 10^{-6}$
Mean error (ms)	11.2	9.99	10.5
Max error (ms)	50.5	50.8	49.5
Computation Time (min)	17.3	20.5	21.1
Breaking condition	Iter	Tol (in 17 iter.)	Iter

A priori state covariance Table 3 presents the results using three different values of *a priori* state covariance: $P_0 = 0.05; 0.20; 0.50 \text{ m}^4/\text{s}^2$. The lower the *a priori* state covariance P_0 , the higher the confidence in the initial state. The results show that according too much confidence in the initial state ($P_0 = 0.05 \text{ m}^4/\text{s}^2$) prevents from reaching the convergence. Conversely, an excessively high *a priori* state covariance forces large variations of the state and would thus lead to an unstable behavior diverging from the solution. P_0 should therefore range between 0.2 and $0.5 \text{ m}^4/\text{s}^2$.

Noise covariance Table 3 also presents the results using three different covariance values: $W_0 = 10^{-4}; 10^{-5}; 10^{-6} \text{ s}^2$. The lower the noise covariance, the higher the confidence in the electrical measurements. Setting an over-confidence in the measurements ($W_0 = 10^{-6} \text{ s}^2$) leads to instabilities in the optimization process, since the range of state samples is strongly widened. However, defining an excessively low covariance ($W_0 = 10^{-4} \text{ s}^2$) slows down the convergence. W_0 should therefore remain close to 10^{-5} s^2 .

Sigma-points In Table 4, all different distributions of sigma-points seem to provide very similar estimations of the conductivities. However, since the number of samples depends on the chosen distribution, the type of sigma-points influences the computation time. The simplex distribution involves $N + 1$ sampling points, thus allowing a shorter computation time compared to the canonical points requiring $2N$ evaluations, where N denotes the number of zones. Regarding efficiency, the use of the simplex distribution outperforms the other cases. From now on, personalizations are carried out using simplex sigma-points.

Number of Regions Our algorithm estimated electrical conductivities of the MS model in regions, computed from the CV information (see Fig. 3(d) to Fig. 3(f)). Here, the influence of the number of regions is studied. For each patient, the method is applied using four and eight CV-based regions.

Table 4: Influence of the distribution of the sigma-points, starting with $X_0 = \{5, 5, 5, 5\} \cdot 10^{-3} \text{ m}^2/\text{s}$ (only on patient 1)

Sigma-Points Distribution	Simplex (N+1)	Canonical (2N)	Star (2N+1) <i>default</i>
Mean error (ms)	10.0	10.0	9.99
Max error (ms)	48.6	50.7	50.8
Computation Time (min)	9.45	16.6	20.5
Breaking condition	Tol (in 13 iter.)	Tol (in 15 iter.)	Tol (in 17 iter.)

Table 5: Influence of the number of zones regarding the error on depolarization times and the ability to virtually reproduce VT, using simplex sigma-points

	Patient 1 (MDT = 58.0 ms)		Patient 2 (MDT = 72.8 ms)		Patient 3 (MDT = 120.0 ms)	
	CV-8	CV-4	CV-8	CV-4	CV-8	CV-4
Zones	CV-8	CV-4	CV-8	CV-4	CV-8	CV-4
Mean error (ms)	10.2	9.99	10.2	8.47	24.3	16.2
Max error (ms)	48.2	50.8	37.7	35.6	97.5	91.6
Computation Time (min)	35.1	9.45	13.0	7.51	14.8	8.48
Breaking condition	Iter	Tol	Tol	Tol	Tol	Tol
Able to reproduce re-entrant VT	✓	✓	✓	✓	×	×

Results are given in Table 5. Using the simplex sigma-points, the use of four zones based on CV gives good results: the convergence is short and the error on depolarization times is low. More regions implies a larger state vector and more sigma-points to compute. Using eight regions does not benefit in term of accuracy, while being more computationally demanding.

2.2 Error on Depolarization Times

In all three clinical cases, a stimulation protocol [13] was performed to trigger the arrhythmia. Due to this pacing, a re-entrant VT was induced for both patient 1 and 2. As for the patient 3, no arrhythmic response was triggered due to the electrical catheter stimulation.

As illustrated in Table 5, the personalized simulations for patient 1 and 2 fit well the recorded depolarization map with a mean error below 10 ms, and even recreate the arrhythmic activity as observed during the VT Stim procedure. Only Relan et al. [9] propose more accurate results (7.1 ms) with the Eikonal model, but the error using the coupled MS model capturing the restitution properties is significantly larger (18.5 ms). Their approach using two coupled electrophysiology models also implies an increased computation time.

For patient 3, the personalization algorithm gives larger errors on the depolarization times (16.2 ms). For this last patient, a re-entrant VT is virtually triggered, whereas no arrhythmic activity was clinically induced. This may be explained by the sparsity of the clinical measurements. This dataset reveals a poor sampling regarding the depolarization map, which makes the personalization hazardous. All three personalizations are illustrated in Fig. 5.

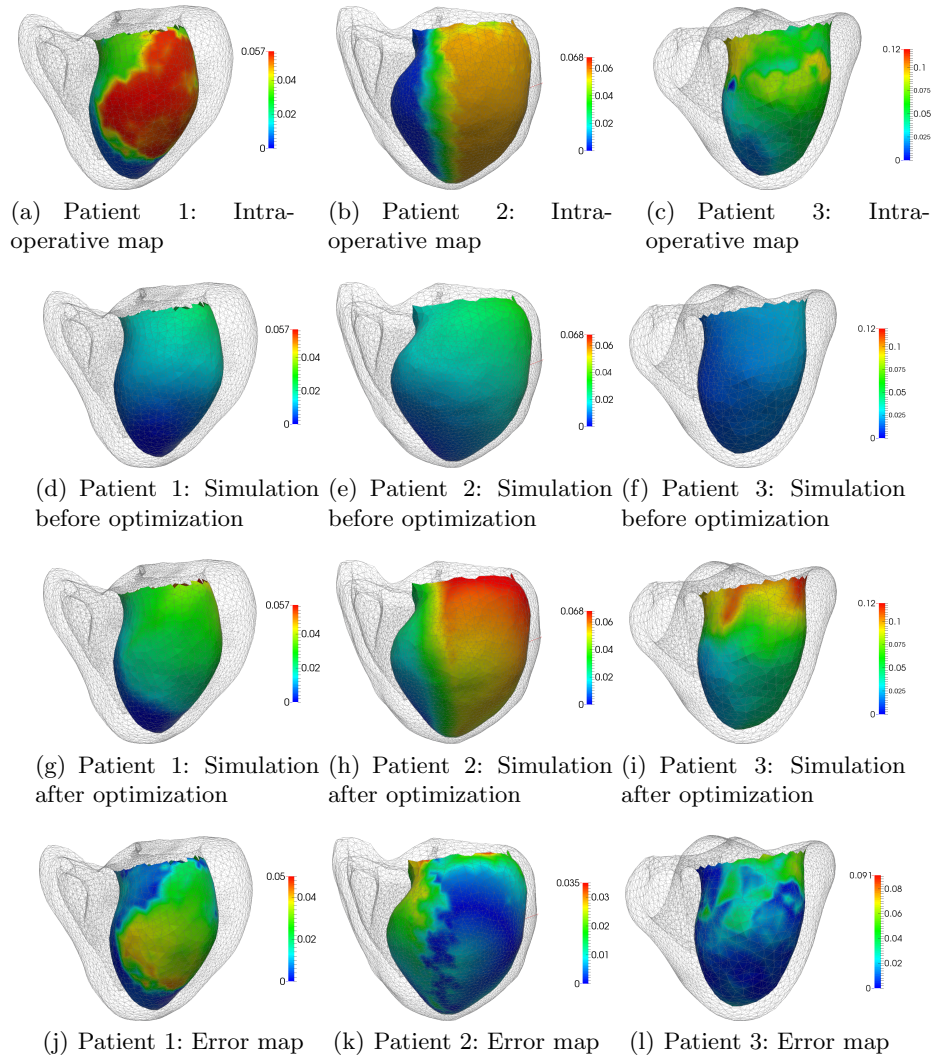


Fig. 5. Comparison of the recorded and simulated map of depolarization times in seconds (before and after personalization) with the resulting error

2.3 Performances

CPU/GPU optimization. We finally propose to compare the performance of the algorithm using the GPU electrophysiology model with a full-CPU version. Using the default parameters and the 4 zones computed from the recorded CV of patient 1, the GPU version runs within 20.5 minutes whereas the CPU version requires 49.1 minutes. The GPU electrophysiology simulation therefore allows

Table 6: Performance results of our three patient-specific electrophysiology simulations

	Patient 1	Patient 2	Patient 3
Personalized regional conductivities (in $10^{-3} \text{ m}^2/\text{s}$)	$x(1) = 0.13$ $x(2) = 0.98$ $x(3) = 5.26$ $x(4) = 5.46$	$x(1) = 0.09$ $x(2) = 1.26$ $x(3) = 3.85$ $x(4) = 4.94$	$x(1) = 0.01$ $x(2) = 0.10$ $x(3) = 0.97$ $x(4) = 4.65$
Time step (s)	$2.50 \cdot 10^{-5}$	$1.05 \cdot 10^{-4}$	$1.85 \cdot 10^{-4}$
Real time ratio	6.57	1.71	0.85

a speedup of only $\times 2.4$ compared to a classical CPU implementation, since the Verdandi library runs on CPU.

Patient-specific simulation After running our algorithm with four zones for each patient, simulations using the personalized regional conductivities are computed. The performance of these patient-specific simulations is detailed in Table 6. Regarding the patient 1, the recorded depolarization is very short (about 58 ms), i.e. the conduction velocity is locally high, which strongly constraints the time step for stability reasons. The resulting simulation presents a performance far from real-time. Patients 2 and 3 have a slower ventricular activation, respectively 72 and 120 ms. The time step can be consequently adapted and both simulation are real-time (patient 3) or close to real-time (patient 2).

3 Conclusion

In this paper, we present an original method to personalize a cardiac electrophysiology model. The electrical conductivities of the model are estimated in regions, related to the intra-operative CV information. Based on an UKF, our algorithm recursively optimizes these conductivities, so that simulated depolarization times match intra-operative measurements. With a GPU version of the electrophysiology model, the personalization requires less than 10 minutes. This outperforms previous works in term of efficiency and could still be improved by implementing the UKF on GPU. For patients 1 and 2, the estimation reaches a mean error below 10 ms regarding the depolarization times. In both cases, the re-entrant VT clinically triggered is successfully induced in the simulation. For patient 3, larger errors are obtained, possibly due to the poor sampling of the recordings.

Applied on only three patients, the method shows very encouraging results. Our algorithm should be tested on more patients, but data are rarely available. Using the personalized electrical conductivities, the patient-specific simulations run in real-time or close to real-time if the depolarization is not too short. Our method therefore completes a personalization framework allowing to create fast patient-specific simulations from clinical data.

References

1. NICE: Arrhythmia - implantable cardioverter defibrillators (icds) (review) (ta95). Clinical report, National Institute for Health and Care Excellence (July 2007)
2. ten Tusscher, K., Noble, D., Noble, P., Panfilov, A.: A model for human ventricular tissue. *American Journal of Physiology - Heart and Circulatory Physiology* **286**(4) (April 2004) 1573–1589
3. Fenton, F., Karma, A.: Vortex dynamics in three-dimensional continuous myocardium with fiber rotation. *Chaos* **8** (1998) 20–47
4. Mitchell, C., Schaeffer, D.: A two-current model for the dynamics of cardiac membrane. *Bulletin of Mathematical Biology* **65** (2003) 767–793
5. Keener, J.: An eikonal-curvature equation for action potential propagation in myocardium. *Journal of Mathematical Biology* **29** (1991) 629–651
6. Zettinig, O., Mansi, T., Georgescu, B., Kayvanpour, E., Sedaghat-Hamedani, F., Amr, A., Haas, J., Steen, H., Meder, B., Katus, H., et al.: Fast data-driven calibration of a cardiac electrophysiology model from images and ecg. In: MICCAI 2013. Springer (2013) 1–8
7. Liu, F., Walmsley, J., Burrage, K.: Parameter estimation for a phenomenological model of the cardiac action potential. *ANZIAM Journal* **52** (2011) C482–C499
8. Chinchapatnam, P., Rhode, K.S., Ginks, M., Rinaldi, C.A., Lambiase, P., Razavi, R., Arridge, S., Sermesant, M.: Model-based imaging of cardiac apparent conductivity and local conduction velocity for diagnosis and planning of therapy. *Medical Imaging, IEEE Transactions on* **27**(11) (2008) 1631–1642
9. Relan, J., Chinchapatnam, P., Sermesant, M., Rhode, K., Ginks, M., Delingette, H., Rinaldi, C.A., Razavi, R., Ayache, N.: Coupled personalization of cardiac electrophysiology models for prediction of ischaemic ventricular tachycardia. *Interface Focus* **1**(3) (2011) 396–407
10. Relan, J., Pop, M., Delingette, H., Wright, G., Ayache, N., Sermesant, M.: Personalisation of a cardiac electrophysiology model using optical mapping and mri for prediction of changes with pacing. *IEEE Transactions on Bio-Medical Engineering* **58**(12) (2011) 3339–3349
11. Camara, O., Pashaei, A., Sebastian, R., Frangi, A.: Personalization of fast conduction purkinje system in eikonal-based electrophysiological models with optical mapping data. In: *Statistical Atlases and Computational Models of the Heart*. Volume 6364 of *Lecture Notes in Computer Science*. Springer Berlin Heidelberg (2010) 281–290
12. Konukoglu, E., Relan, J., Cilingir, U., Menze, B.H., Chinchapatnam, P., Jadidi, A., Cochet, H., Hocini, M., Delingette, H., Jaïs, P., et al.: Efficient probabilistic model personalization integrating uncertainty on data and parameters: Application to eikonal-diffusion models in cardiac electrophysiology. *Progress in Biophysics and Molecular Biology* **107**(1) (2011) 134–146
13. Wellens, H.J., Brugada, P., Stevenson, W.G.: Programmed electrical stimulation of the heart in patients with life-threatening ventricular arrhythmias: What is the significance of induced arrhythmias and what is the correct stimulator protocol? *Circulation* **72**(1) (1985) 1–7
14. Talbot, H., Marchesseau, S., Duriez, C., Sermesant, M., Cotin, S., Delingette, H.: Towards an interactive electromechanical model of the heart. *Journal of the Royal Society Interface Focus* **3**(2) (April 2013)
15. Julier, S.J., Uhlmann, J.K., Durrant-Whyte, H.F.: A new approach for filtering nonlinear systems. In: *American Control Conference, Proceedings of the 1995*. Volume 3., IEEE (1995) 1628–1632